

# The Physiological Significance of the Time-to-Maximum (Tmax) Parameter in Perfusion MRI

Fernando Calamante, PhD; Søren Christensen, PhD; Patricia M. Desmond, MD, FRANZCR;  
Leif Østergaard, MD, PhD; Stephen M. Davis, MD, FRACP; Alan Connelly, PhD

**Background and Purpose**—Many perfusion-related MRI parameters are used to investigate the penumbra in stroke. Although time-to-maximum (Tmax) of the residue function has been suggested as a very promising parameter, its physiological meaning and sensitivity to experimental conditions are not well-understood.

**Methods**—We used simulations to further our understanding of the practical meaning of Tmax and to provide recommendations for its use in clinical investigations. We interpret in vivo examples guided by the simulation findings.

**Results**—Whereas Tmax has several attractive properties for clinical use, it is shown that its physiological interpretation is complex and affected by experimental conditions. Tmax is found to reflect a combination of delay, dispersion, and, to a lesser degree, mean transit time. It should therefore mainly be considered a measure of macrovascular characteristics. Furthermore, based on the simulations, use of temporal-interpolation is highly recommended, as is correction for slice-acquisition timing differences.

**Conclusion**—Special care should be taken when setting-up Tmax thresholds for data acquired with different protocols (eg, multicenter studies) because various factors can influence the measured Tmax. Because of its complementary information, used in conjunction with delay-insensitive cerebral blood-flow, cerebral blood volume, and mean transit time maps, Tmax should provide important additional information on brain hemodynamic status. (*Stroke*. 2010;41:1169-1174.)

**Key Words:** magnetic resonance imaging ■ perfusion ■ stroke

The role of diffusion and perfusion MRI for the identification of patients with stroke who are most suited for thrombolysis is an active area of research. However, there is still no consensus regarding the specific perfusion parameter and optimal analysis method that best identify the penumbra. The most commonly used perfusion parameters include cerebral blood flow (CBF), cerebral blood volume (CBV), and mean transit time (MTT). Recently, an increasing number of studies have promoted the use of Tmax (the time to maximum of the residue function obtained by deconvolution).<sup>1-5</sup> Tmax has been used in recent clinical trials<sup>3,4</sup> and will be in the inclusion criteria in the forthcoming DEFUSE-2 and EXTEND trials. Despite a complex interaction of many factors influencing the measured Tmax, there has been no detailed investigation of its pathophysiological meaning or its sensitivity to the experimental conditions.

The tissue contrast agent concentration [ $C(t)$ ] can be expressed as a convolution of the arterial input function (AIF) and the residue function [ $R(t)$ ]:<sup>6</sup>

$$(1) \quad C(t) = \text{CBF} \times (\text{AIF}(t) \otimes R(t))$$

The residue function is obtained by deconvolution and its maximum value occurs, by definition, at Tmax. Therefore, Tmax is theoretic-

ally the arrival delay between the AIF and  $C(t)$  (Figure 1; after deconvolution,  $t=0$  corresponds to the AIF arrival time).

However, other factors can influence Tmax in practice. For example, patients with arterial abnormalities often exhibit bolus temporal dispersion,<sup>7</sup> which distorts the shape of the calculated  $R(t)$  to a more peaked shape (Figure 1).<sup>8</sup> In these cases, Tmax will not only measure delay but also will be affected (in a complex manner) by the degree of dispersion. A further practical factor that can influence Tmax is the deconvolution analysis itself. To minimize the high sensitivity to noise, deconvolution is combined with a filtering technique (so-called regularization),<sup>9</sup> which smoothes  $R(t)$  and introduces oscillations in its shape (Figure 1).<sup>8</sup> These deconvolution-related distortions will influence the measured Tmax. In addition, because the optimum degree of regularization depends on factors such as MTT, CBV, and signal-to-noise ratio (SNR), these can also affect Tmax in practice.

Because of all these factors, the physiological meaning of Tmax is not straightforward. In this study we performed simulations to investigate the influence of Tmax on tissue and vascular parameters, experimental conditions, and analysis methods. The aim of the in silico part of the study is to further our understanding of the practical meaning of Tmax, to provide a quantitative assessment of the factors that influence

Received February 1, 2010; accepted February 27, 2010.

From Brain Research Institute (F.C., A.C.), Florey Neuroscience Institutes (Austin), Melbourne, Australia; Department of Medicine (F.C., A.C.), Austin Health and Northern Health, University of Melbourne, Melbourne, Australia; Department of Radiology (S.C., P.D.), Royal Melbourne Hospital, University of Melbourne, Melbourne, Australia; Department of Neurology (S.C., S.M.D.), Royal Melbourne Hospital, University of Melbourne, Melbourne, Australia; and Center for Functionally Integrative Neuroscience (L.Ø.), Århus University Hospital, Århus, Denmark.

Correspondence to Fernando Calamante, PhD, Brain Research Institute, Neurosciences Building, Austin Health, Banksia Street, Heidelberg West, Victoria 3081, Australia. E-mail fercala@brain.org.au

© 2010 American Heart Association, Inc.

Stroke is available at <http://stroke.ahajournals.org>

DOI: 10.1161/STROKEAHA.110.580670

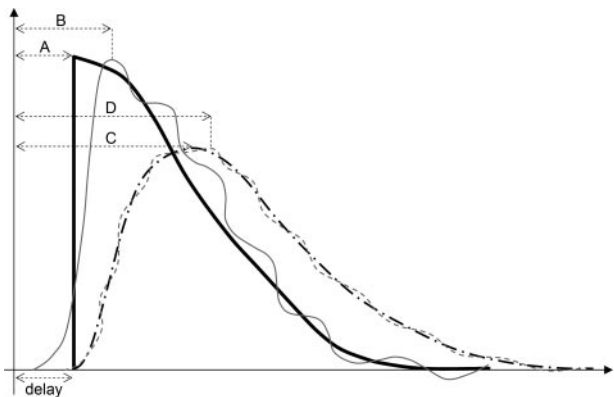


**Figure 1.** Schematic examples of theoretical and measured residue functions. Thick, solid, black line, Ideal residue function in the presence of delay (A, arrow indicates theoretical Tmax). Solid gray line, Corresponding function including distortions introduced by deconvolution (B, arrow indicates measured Tmax). Dash/dot black line, Case in the presence of delay and dispersion (C, arrow indicates measured Tmax). Dashed gray line, Corresponding function including the deconvolution-related distortions (D, arrow indicates measured Tmax). Tmax corresponds to delay only in the ideal case.

its measurement, and to provide recommendations for its clinical use. In vivo examples are presented to illustrate the conclusions from the simulation findings in real data.

### Materials and Methods

#### In Silico Data

Data were simulated using well-established methods.<sup>8,9</sup> In brief, the AIF was modeled as a  $\gamma$ -variate function<sup>9</sup>:  $AIF(t) = A_0 \times t^r \times \exp(-t/b)$ .

To investigate the influence of AIF on Tmax, 2 cases were considered: a “typical” AIF ( $r=3; b=1.5$ )<sup>9</sup> and a wider version ( $r=3.25; b=1.75$ ). The scaling constants were chosen to simulate signal intensity decreases observed for normal gray matter ( $\approx 40\%$ ). Two  $R(t)$  models were considered, single-exponential and linear models,<sup>9</sup> with MTT of 4 to 14 seconds (1-second increments), for each of 2 CBV cases (2% and 4%). Delay was modeled by shifting the tissue concentration curves, with delays ( $d$ ) between  $-4$  and  $+4$  seconds in 0.5-second increments ( $d=0$  corresponds to AIF and tissue curves aligned). Bolus dispersion was modeled using an exponential vascular transport function<sup>10</sup>:  $VTF(t) = \exp(-t/D)/D$ , where the dispersion parameter  $D=1,2,3,4$  seconds. Gaussian noise was added to the tissue signal intensity time courses (SNR=10, 50, 200; corresponding to low, typical, and high SNR, respectively). Simulations were performed for gradient echo sequences (echo time [TE]=50 ms; repetition time [TR]=1 to 2.5 seconds, in 0.5-second increments). For simplicity,  $T_1$  relaxation effects were not included.<sup>11</sup>

#### Simulations: Data Analysis

Deconvolution was performed using oscillation index regularized block-circulant singular value decomposition (oSVD) (which produces delay-insensitive CBF and MTT values),<sup>12</sup> with 2 levels of regularization: oscillation index (OI)=0.085 and 0.095. To allow interpretation of historical data, some results are also reported for singular value decomposition (SVD),<sup>9</sup> with 3 levels of regularization: SVD threshold  $P_{SVD}=5,10,20\%$ . Tmax was calculated from the time-to-maximum of the deconvolved residue function.<sup>1</sup> To investigate the effect of discretization errors (attributable to data sampling at TR intervals), Tmax was also calculated after temporal interpolation of the calculated  $R(t)$ : interpolated to TR/4 using Fourier domain interpolation.<sup>13</sup> For each condition, 1000 noise realizations were performed.

To investigate the influence of the various factors that affect the measured Tmax, regression models with terms delay ( $d$ ), dispersion

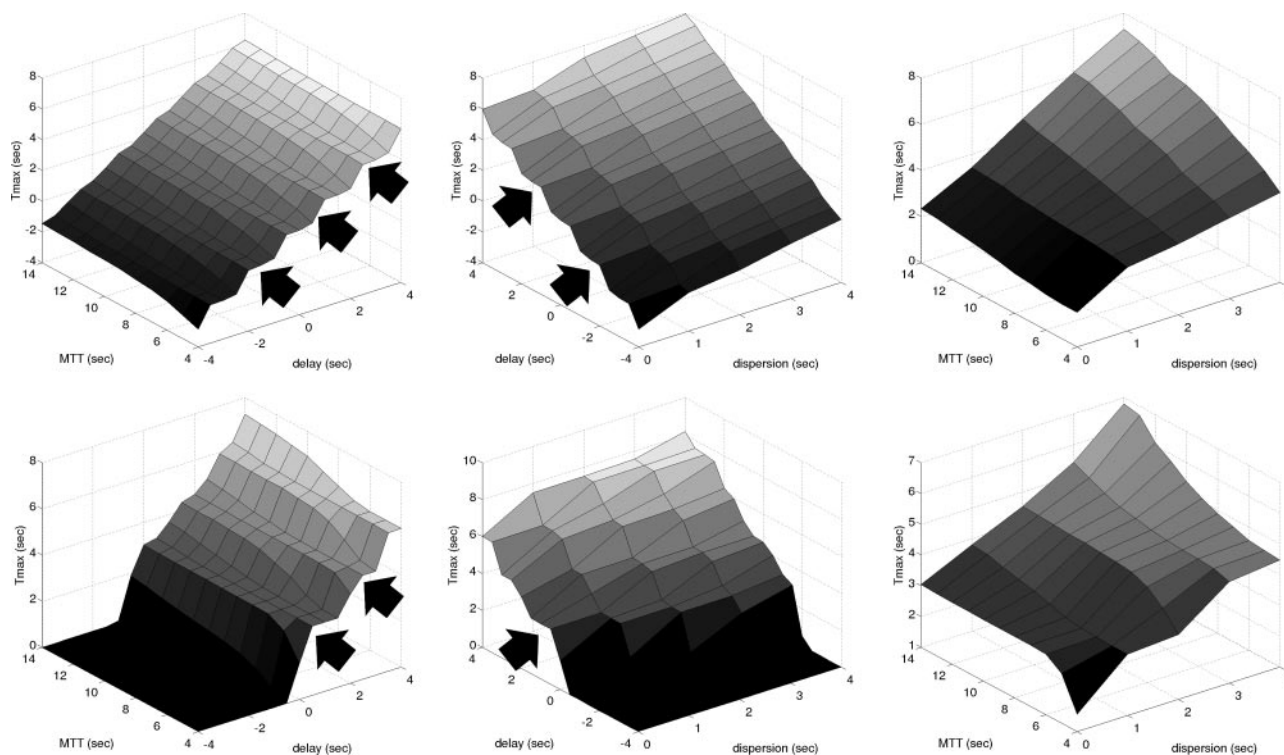


**Figure 2.** Measured Tmax values for data simulated using a typical AIF, exponential residue function, CBV=4%, SNR=high, TR=1.5 seconds, and no temporal interpolation. Left, Tmax as a function of delay and MTT for fixed dispersion ( $D=0$  seconds). Middle, Tmax as a function of delay and dispersion for fixed MTT (MTT=4 sec). Right, Tmax as a function of dispersion and MTT for fixed delay ( $d=0$  seconds). Top row, Tmax values calculated using oSVD (OI=0.095). Bottom row, Values calculated using SVD ( $P_{SVD}=10\%$ ). The measured Tmax increases with increasing delay, dispersion, or MTT, although with different sensitivity to changes in these parameters.

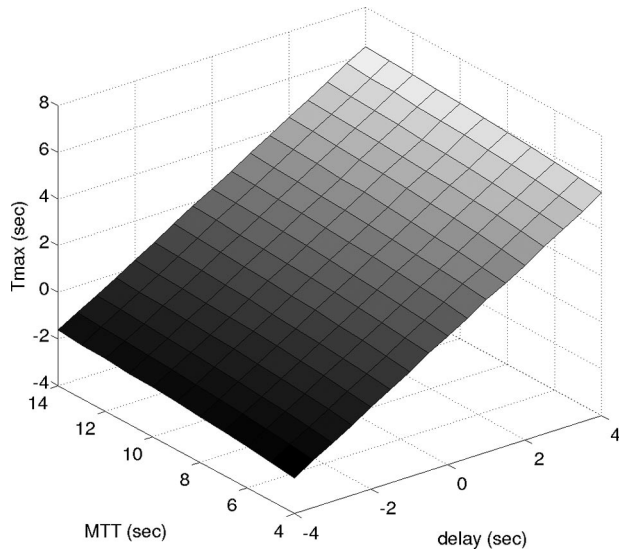


**Figure 3.** Measured Tmax values with oSVD (OI=0.095) and calculated after temporal interpolation. The plot shows Tmax as a function of delay and MTT for fixed dispersion ( $D=0$  seconds). Data are the same as that in Figure 2 top left, except for the use of temporal interpolation.

( $D$ ), and MTT were used (other factors, eg, TR, SNR, were kept constant for each regression). Because SVD has now been superseded by its delay-insensitive version oSVD,<sup>12</sup> regression analyses were only performed for the latter. Based on a preliminary analysis, a linear relationship was sufficient for delay and MTT, but a nonlinear effect was observed with dispersion. Similarly, interaction-effect MTT dispersion was detected. Therefore, the following model was considered suitable:

$$(2) \quad \text{Tmax} = C_0 + C_d \cdot d + C_{MTT} \cdot \text{MTT} + C_D \cdot D + C_{D^2} \cdot D^2 + C_{MTT \times D} \cdot \text{MTT} \times D + C_{MTT \times D^2} \cdot \text{MTT} \times D^2$$

where the various  $C$  are the coefficients of the regression (eg,  $C_d$  is the linear-dependency on delay,  $C_{D^2}$  is the quadratic term on dispersion,  $C_{MTT \times D}$  is the interaction term between MTT and dispersion, etc). Note that MTT in equation 2 indicates the true value and not the measured value.

**In Vivo Data**

To illustrate the results from the simulations, data are shown from 2 acute stroke patients (labeled P1 and P2). Time-to-onset/National Institutes of Health Stroke Scale scores were 4 hours and 55 minutes/19 for P1 and 1 hour and 45 minutes/10 for P2. In both cases, the neurological deficits were stable before MR scanning, which was performed before thrombolysis. Both patients had a right internal carotid artery occlusion. Perfusion data were acquired at 3 T, with TR of 1.5 seconds and 0.1 mmol/kg bolus of contrast agent (injection rate=5 mL/sec). The AIF was measured from the contralateral middle cerebral artery. All maps were calculated using oSVD (OI=0.095). Informed consent was obtained from all patients and the study was approved by the local ethics committee.

**Results**

**In Silico Data**

Figure 2 shows representative results obtained using oSVD (top row) and SVD (bottom row). The plots show the dependency of Tmax on 2 of the 3 remaining variables (delay, dispersion, and simulated MTT) when the third one is kept at a constant value. SVD gave similar results to oSVD, with the obvious exception that SVD does not allow for negative

**Table. Regression Coefficients**

Simulated Conditions						
	AIF, Type	$R(t)$ , Type	CBV, %	TR, sec	SNR	OI
1	Typical	Exponential	4	1	High	0.095
2	Typical	Exponential	4	1.5	High	0.095
3	Typical	Exponential	4	2	High	0.095
4	Typical	Exponential	4	2.5	High	0.095
5	Typical	Exponential	2	1	High	0.095
6	Wider	Exponential	4	1	High	0.095
7	Typical	Linear	4	1	High	0.095
8	Typical	Exponential	4	1	Normal	0.095
9	Typical	Exponential	4	1	Low	0.095
10	Typical	Exponential	4	1	Normal	0.085

Coefficients of the regression model (columns 8–14) for various simulated conditions (columns 1–7). See equation 2 for more details regarding the coefficients. The mean values with their 95% confidence intervals. The last column lists the corresponding  $r^2$  statistic.

Tmax (a zero value is found).<sup>12</sup> Visual inspection of the surface plots shows all 3 variables influence the measured Tmax, with bolus delay having the largest influence (ie, steepest slope), followed by bolus dispersion and, finally, a small dependency on MTT. This Tmax dependency represents a typical result, and the trends were qualitatively similar for the other simulated cases (data not shown).

As shown in Figure 2 (left and middle columns), the TR sampling of bolus tracking data leads to discretization errors in Tmax as a function of delay (particularly for small dispersion or short MTT; arrows). Because the measured Tmax can only take discrete values (multiples of TR), a “staircase” effect is observed. As expected, this effect increased with increasing TR (data not shown). This “staircase” artifact was eliminated by  $R(t)$  interpolation before Tmax calculation (Figure 3).

To quantify all these effects, the Table shows the regression coefficients for various typical combinations of simulated conditions. Results are shown for Tmax values calculated after temporal interpolation; similar coefficients were observed without interpolation (data not shown). The measured Tmax is highly influenced by delay ( $C_d \approx 1$ ) to a slightly lesser degree by dispersion ( $C_D \approx 0.85$ ) and only moderately by MTT ( $C_{MTT} \approx 0.1$ ). Furthermore, the higher-order terms (ie, the interaction and quadratic terms) have only a mild-to-moderate contribution.

The comparison of coefficients from various simulated conditions shows the contribution from delay ( $C_d$ ) is relatively constant. The delay has a simple additive effect on Tmax, regardless of the simulated condition. The contribution from dispersion ( $C_D$ ) is influenced primarily by TR (compare rows 1 to 4 in the Table) and, to a smaller degree, by AIF (rows 1 and 6), CBV (rows 1 and 5) and SNR (rows 1,8,9). The contribution from MTT ( $C_{MTT}$ ) is primarily influenced by SNR and, to a smaller degree, by AIF and  $R(t)$  (rows 1 and 7). The quadratic dispersion contribution ( $C_{D^2}$ ) is slightly influenced by TR, AIF, and SNR.

The only condition that leads to different coefficients is SNR. The dependency was different for low SNR, with much higher contributions from MTT and dispersion to the measured Tmax (Figure 4).

Table. Continued

Regression Results							
$C_0$	$C_d$	$C_{MTT}$	$C_D$	$C_D^2$ (1/sec)	$C_{MTT \times D}$ (1/sec)	$C_{MTT \times D^2}$ (1/s <sup>2</sup> )	$r^2$
1.101 (1.065–1.137)	0.998 (0.995–1.000)	0.075 (0.072–0.079)	0.740 (0.694–0.780)	-0.069 (-0.079–-0.059)	0.054 (0.049–0.058)	0.005 (0.004–0.006)	0.999
1.322 (1.294–1.351)	1.000 (0.998–1.002)	0.075 (0.072–0.078)	0.789 (0.756–0.823)	-0.109 (-0.117–-0.101)	0.023 (0.020–0.027)	0.011 (0.010–0.012)	0.999
1.500 (1.477–1.523)	1.002 (1.000–1.003)	0.086 (0.084–0.089)	0.952 (0.925–0.979)	-0.149 (-0.155–-0.142)	-0.001 (-0.004–0.002)	0.013 (0.012–0.013)	0.999
1.773 (1.747–1.799)	1.003 (1.001–1.005)	0.091 (0.088–0.094)	0.919 (0.889–0.950)	-0.124 (-0.131–-0.116)	0.004 (0.001–0.007)	0.007 (0.006–0.008)	0.999
1.135 (1.103–1.167)	0.996 (0.994–0.999)	0.101 (0.097–0.104)	0.806 (0.768–0.844)	-0.086 (-0.095–-0.077)	0.044 (0.040–0.048)	0.006 (0.005–0.007)	0.999
1.181 (1.149–1.214)	0.997 (0.995–0.999)	0.097 (0.094–0.101)	0.820 (0.782–0.858)	-0.089 (-0.098–-0.079)	0.041 (0.037–0.045)	0.007 (0.006–0.008)	0.999
1.121 (1.063–1.180)	0.997 (0.993–1.001)	0.094 (0.088–0.100)	0.754 (0.685–0.823)	-0.076 (-0.092–-0.059)	0.092 (0.085–0.099)	0.001 (-0.001–0.002)	0.998
1.105 (1.072–1.139)	0.993 (0.991–0.996)	0.155 (0.152–0.159)	0.879 (0.839–0.918)	-0.094 (-0.104–-0.085)	0.040 (0.036–0.044)	0.007 (0.006–0.008)	0.999
-2.015 (-2.226–-1.803)	0.852 (0.839–0.866)	1.159 (1.136–1.181)	1.320 (1.070–1.571)	0.058 (-0.002–0.118)	0.016 (-0.010–0.043)	-0.004 (-0.010–0.002)	0.988
1.165 (1.133–1.196)	0.995 (0.993–0.997)	0.147 (0.143–0.150)	0.883 (0.846–0.920)	-0.096 (-0.104–-0.087)	0.037 (0.033–0.040)	0.007 (0.006–0.008)	0.999

By varying TR (Table and Figure 4), the offset term of the regression ( $C_0$ ) is modified (even after temporal interpolation). The offset term is also affected (although mildly) by the degree of regularization  $\text{OI}$ .

Although  $T_{\text{max}}$  is calculated after deconvolution analysis, there was a small residual effect of AIF on the measured  $T_{\text{max}}$ . This was primarily seen as a change in the offset term of the regression and in the dispersion and MTT contributions (Table).

**In Vivo Data**

The in vivo examples clearly illustrate the nontrivial relationship between  $T_{\text{max}}$  and MTT (Figure 5). In particular, P1 shows an example in which  $T_{\text{max}}$  and MTT identify abnormalities of similar extent and severity. P2, however, shows an example of severe  $T_{\text{max}}$  lesion in the presence of mild MTT abnormality. For completeness, CBF and CBV maps are also shown (for display purposes, these maps were scaled by setting normal white matter CBF to 22 mL/100 g/min).<sup>9</sup>

**Discussion**

This study used in silico data to characterize the dependency of  $T_{\text{max}}$  on physiological and experimental parameters, as well as on various analysis methods. It was shown that whereas  $T_{\text{max}}$  theoretically reflects bolus delay, the mea-

sured  $T_{\text{max}}$  is influenced also by bolus temporal dispersion and, to a smaller degree, by MTT. This suggests the physiological interpretation of  $T_{\text{max}}$  in stroke is not straightforward, because various hemodynamic scenarios can lead to the same  $T_{\text{max}}$  appearance. For example, prolonged  $T_{\text{max}}$  can represent normal perfusion but with delayed bolus arrival or tissue with dispersion and increased MTT (Figure 5). These 2 situations cannot be distinguished based on  $T_{\text{max}}$  alone. Note, however, that given the modest dependency on MTT (Figure 2), it is unlikely that a severe  $T_{\text{max}}$  abnormality could be solely explained by prolonged MTT, and it is likely that this case reflects also delay or dispersion. In contrast, MTT provides, in principle, easier physiological interpretation; it is believed to be inversely proportional to perfusion pressure<sup>14</sup> (note, however, it could be also influenced by dispersion).<sup>10</sup> Therefore, when a physiological interpretation of the abnormality is required,  $T_{\text{max}}$  should not be considered on its own; by combining with other macrovascular (eg, an alternative measure of bolus delay) or microvascular information (eg, MTT), the various factors contributing to the measured  $T_{\text{max}}$  may be disentangled. In fact,  $T_{\text{max}}$  provides different information to that contained in CBF, CBV, and MTT maps, and its main strength may be when combined with these other

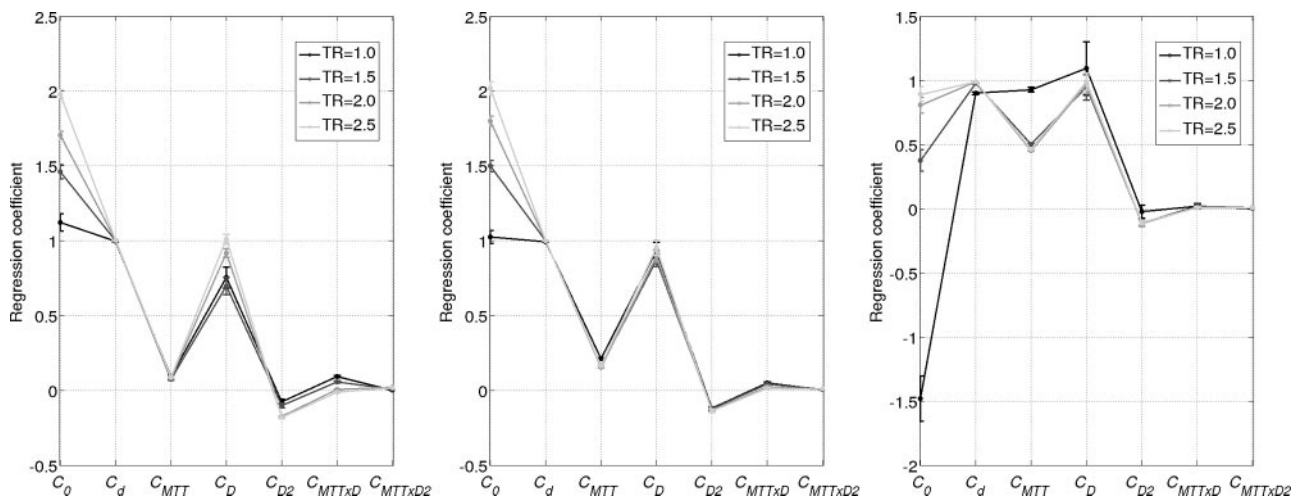


**Figure 4.** Coefficients of the regression for various TR. Left, High SNR. Middle, Normal SNR. Right, Low SNR. The x-axis indicates the various terms in the regression model (equation 2). Data simulated using the typical AIF, linear residue function, CBV=4%, and  $T_{\text{max}}$  calculated after temporal interpolation. Note different y-axis scale in low SNR graph.

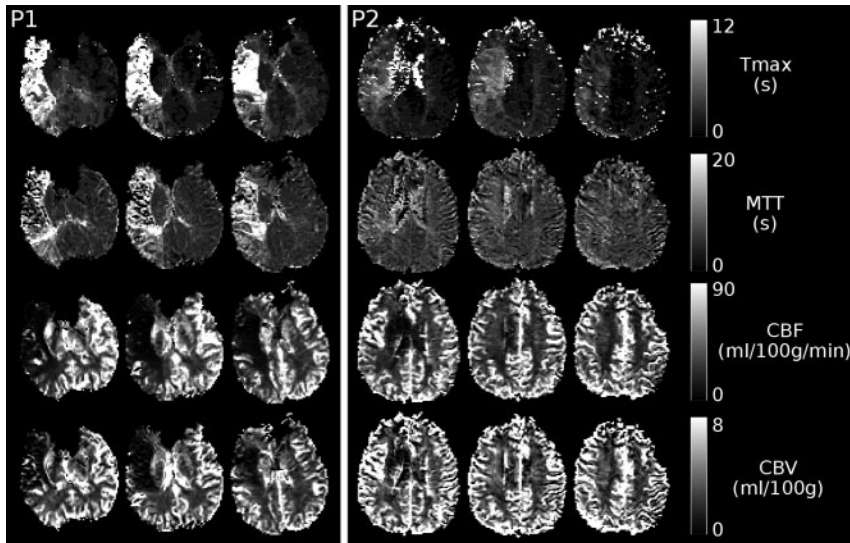


**Figure 5.** In vivo data (3 slices are shown for each case). Top row, MTT. Second row, Tmax. Third row, CBF. Bottom row, CBV.

parameters. This is particularly the case when a delay-insensitive deconvolution algorithm is used (as is now increasingly common). These hemodynamic maps provide complementary information that can be best exploited using predictor models<sup>15</sup> in which the relevance of each parameter to infarct prediction is determined by a training data set.

The presence of delay/dispersion are often unavoidable<sup>7</sup> because of the difficulty in measuring the AIF from small distal arteries. The dependency on delay and dispersion (increased Tmax with increasing delay/dispersion) was theoretically expected. Both effects lead to a delayed maximum of the measured residue function (Figure 1). Tmax was also found to increase with prolonged MTT, a more complex effect related to the deconvolution. It is introduced by the filtering properties of the regularization process and explains, for example, the dependency of  $C_{MTT}$  on OI and SNR (known to influence the regularization).

The notion that Tmax and, hence, delay are useful predictors in stroke is controversial. Delay could be considered a nuisance parameter, and scenarios exist in which delay is unrelated to flow, eg, in chronic conditions with sufficient collateral supply. In these situations, it could be argued that Tmax should not be used because it can lead to misleading conclusions. Despite these reservations, there is now empirical evidence that heavily delay-weighted measures provide useful information.<sup>5</sup> It could be speculated the high Tmax values seen in hyperacute stroke often coexist with hypoperfusion and indicate poor delayed collateral supply. It is conceivable that regions with long arrival delay, even if relatively well-perfused, are the most at risk if perfusion pressure further declines. More research into the temporal dynamics of blood supply and collaterals recruitment is needed to understand the significance of delay in stroke.<sup>16,17</sup>

The TR sampling of perfusion data leads to discretization errors in the measured Tmax (ie, the measured Tmax is rounded-off to a value multiple of TR). This coarse discretization could have important implications in clinical studies. For example, when a threshold is used to define hypoperfusion, rounding-off effects could lead to variations in the hypoperfused area. This effect is most significant when the threshold is comparable to

TR, as in the initial Tmax >2-second studies.<sup>2-4</sup> These rounding errors could also have a deleterious effect in multicenter studies in which data are often acquired with different TR. For example, Figure 4 shows a TR-related doubling of the offset term  $C_0$  for normal SNR (from 1 to 2 seconds), making the Tmax measurement TR-dependent. Because temporal interpolation was shown to eliminate discretization errors, its use is highly recommended. However, because of the small remaining TR sensitivity (through the offset term), it is important that multicenter studies should select a fixed TR. Furthermore, being sensitive to delay, Tmax is also sensitive to the timing differences of slices during acquisition (in fact, this extra delay can affect Tmax between slices by up to 1 TR). It is therefore essential that these timing differences are appropriately accounted for during Tmax computation. In this way, the variability in Tmax quantification that is under user control will be minimized.

From all conditions simulated, SNR was the only parameter that led to different trends (Figure 4). In particular, low SNR data made Tmax measurements more sensitive to MTT. This is likely attributable to a suboptimal OI (the OI used were optimal for normal-to-high SNR).<sup>12</sup> Physiological interpretation of Tmax will be different if a suboptimal regularization level is used. This could have implications for multicenter studies. The optimal level of regularization is known to depend on many factors, eg, contrast-to-noise ratio, TR, and so on.<sup>8,12</sup> Therefore, if a fixed level of regularization is used during deconvolution, a given Tmax threshold could identify different areas of hypoperfusion for data acquired with different sequence parameters, injection protocol, and so on. More generally, optimal Tmax thresholds from one study must be used with caution in other studies if the same experimental conditions are not ensured. For example, a different SNR, TR, deconvolution algorithm, or image resolution could render the suggested Tmax threshold suboptimal.

Consistent with the predictions of the in silico data, the in vivo examples clearly show the complex relationship between Tmax and MTT, and that Tmax primarily reflects macrovascular features. The relative contributions of delay, dispersion, and MTT to the measured Tmax and MTT values therefore explain their differences in Figure 5. For example,

based on the simulations, an MTT abnormality will always affect Tmax (although with modest weight). In contrast, the similar Tmax and MTT abnormalities in P1 suggest that the severe Tmax prolongation likely reflects a contribution also from delay or dispersion (this interpretation would not have been possible with the Tmax map in isolation or without the simulation findings). However, the mild MTT abnormality in P2 (but with a severe Tmax lesion) probably suggests a case in which sufficient collateral supply exists to maintain microvascular integrity; ie, the Tmax abnormality reflects almost only delay/dispersion and not MTT prolongation (benign oligemia), consistent with the simulation findings that Tmax primarily reflects macrovascular features. The in vivo examples are consistent with the simulation findings and emphasize the complementary information contained in Tmax and MTT; for example, the hemodynamic disturbance indicated by the asymmetrical Tmax pattern in P2 could not have been inferred from CBF, CBV, and MTT maps alone.

Despite its complex physiological interpretation, Tmax has a number of useful practical features. First, because Tmax can be determined from a limited number of sampling points at the beginning of the bolus, it may be less sensitive than MTT to patient motion. MTT quantification needs a greater amount of usable data (for determination of CBV, which is needed in MTT calculation). Second, if extremely long bolus delay/dispersion are present, CBV may be underestimated (and MTT overestimated) when insufficient data points are acquired.<sup>10</sup> However, Tmax is less sensitive to this effect (because it depends on fewer measurements). Third, like MTT, it is approximately uniform across normal gray and white matter, which is beneficial for visual conspicuity and when maps are thresholded. Fourth, depending on the analysis software used, there is a further possible practical advantage. When there is low contrast delivery to a brain region and CBV is approximately 0, the region may appear as a “black hole” in MTT maps, although it may not affect the Tmax map.<sup>2</sup> This effect can often disturb interpretation of MTT abnormalities, possibly contributing to the increased popularity of Tmax. However, this “artifact” is most commonly related to software implementation (eg, it can be avoided by setting the intensity in those regions to the maximum MTT value). Regions experiencing no tracer arrival can also be caused by insufficient sampling time to cover the entire bolus.

### Conclusion

Tmax is a parameter with several attractive properties for clinical use, although its physiological interpretation is complex and affected by experimental conditions. Tmax reflects a combination of delay, dispersion, and, to a lesser degree, MTT; therefore, it mainly should be considered a measure of macrovascular features. It is highly recommended that temporal interpolation be used before Tmax computation and that the slice-acquisition timing differences be accounted for; this should minimize sources of interstudy variability that are under user control. Special care should be taken when setting-up Tmax thresholds for data acquired with different protocols (eg, in multicenter studies) because various factors can influence the measured Tmax. Because of its complementary information used in conjunction with delay-

insensitive CBF, CBV, and MTT maps, Tmax will provide important additional information on cerebral hemodynamics.

### Sources of Funding

F.C. and A.C. were supported by the National Health and Medical Research Council (NHMRC) of Australia and Austin Health. L.Ø. was supported by the Danish National Research Foundation.

### Disclosures

None.

### References

1. Kidwell CS, Saver JL, Mattiello J, Starkman S, Vinuela F, Duckwiler G, Gobin YP, Jahan R, Vespa P, Kalafut M, Alger JR. Thrombolytic reversal of acute human cerebral ischemic injury shown by diffusion/perfusion MRI. *Ann Neurol*. 2000;47:462–469.
2. Butcher KS, Parsons M, MacGregor L, Barber PA, Chalk J, Bladin C, Levi C, Kimber T, Schultz D, Fink J, Tress B, Donnan G, Davis S; EPITHET Investigators. Refining the perfusion-diffusion mismatch hypothesis. *Stroke*. 2005;36:1153–1159.
3. Albers GW, Thijs VN, Wechsler L, Kemp S, Schlaug G, Skalabrin E, Bammer R, Kakuda W, Lansberg MG, Shuaib A, Coplin W, Hamilton S, Moseley M, Marks MP. MRI profiles predict clinical response to early reperfusion: The Diffusion-Perfusion Imaging Evaluation for Understanding Stroke Evolution (DEFUSE) study. *Ann Neurol*. 2006;60:508–517.
4. Davis SM, Donnan GA, Parsons MW, Levi C, Butcher KS, Peeters A, Barber PA, Bladin C, De Silva DA, Byrnes G, Chalk JB, Fink JN, Kimber TE, Schultz D, Hand PJ, Frayne J, Hankey G, Muir K, Gerraty R, Tress BM, Desmond PM. Effects of alteplase beyond 3h after stroke in the Echoplanar Imaging Thrombolytic Evaluation Trial (Epithet): A placebo-controlled randomised trial. *Lancet Neurol*. 2008;7:299–309.
5. Olivot JM, Mlynash M, Thijs VN, Kemp S, Lansberg MG, Wechsler L, Bammer R, Marks MP, Albers GW. Optimal Tmax threshold for predicting penumbral tissue in acute stroke. *Stroke*. 2009;40:469–475.
6. Calamante F, Thomas DL, Pell GS, Wiersma J, Turner R. Measuring cerebral blood flow using magnetic resonance techniques. *J Cereb Blood Flow Metab*. 1999;19:701–735.
7. Calamante F, Willats L, Gadian DG, Connelly A. Bolus delay and dispersion in perfusion MRI: implications for tissue predictor models in stroke. *Magn Reson Med*. 2006;55:1180–1185.
8. Calamante F, Gadian DG, Connelly A. Quantification of bolus-tracking MRI: Improved characterization of the tissue residue function using Tikhonov regularization. *Magn Reson Med*. 2003;50:1237–1247.
9. Østergaard L, Weisskoff RM, Chesler DA, Gyldensted C, Rosen BR. High-resolution measurement of cerebral blood flow using intravascular tracer bolus passages. Part-I. *Magn Reson Med*. 1996;36:715–725.
10. Calamante F, Gadian DG, Connelly A. Delay and dispersion effects in dynamic susceptibility contrast MRI: simulations using singular value decomposition. *Magn Reson Med*. 2000;44:466–473.
11. Calamante F, Vonken EJ, van Osch MJ. Contrast agent concentration measurements affecting quantification of bolus-tracking perfusion MRI. *Magn Reson Med*. 2007;58:544–553.
12. Wu O, Østergaard L, Weisskoff RM, Benner T, Rosen BR, Sorensen AG. Tracer-arrival timing-insensitive technique for estimating flow in MR perfusion-weighted imaging using singular value decomposition with a block-circulant deconvolution matrix. *Magn Reson Med*. 2003;50:164–174.
13. Salluzzi M, Frayne R, Smith MR. Is correction necessary when clinically determining quantitative cerebral perfusion parameters from multi-slice dynamic susceptibility contrast MR studies? *Phys Med Biol*. 2006;51:407–424.
14. Schumann P, Touzani O, Young AR, Morello R, Baron JC, MacKenzie ET. Evaluation of the ratio of cerebral blood flow to cerebral blood volume as an index of local cerebral perfusion pressure. *Brain*. 1998;121:1369–1379.
15. Wu O, Koroshetz WJ, Østergaard L, Buonanno FS, Copen WA, Gonzalez RG, Rordorf G, Rosen BR, Schwamm LH, Weisskoff RM, Sorensen AG. Predicting tissue outcome in acute human cerebral ischemia using combined diffusion- and perfusion-weighted MRI. *Stroke*. 2001;32:933–942.
16. Liebeskind DS. Collaterals in acute stroke: beyond the clot. *Neuroimaging Clin N Am*. 2005;15:553–573.
17. Christensen S, Calamante F, Hjort N, Wu O, Blankholm AD, Desmond P, Davis S, Østergaard L. Inferring origin of vascular supply from tracer arrival timing patterns using Bolus Tracking MRI. *J Magn Reson Imaging*. 2008;27:1371–1381.

## The Physiological Significance of the Time-to-Maximum (Tmax) Parameter in Perfusion MRI

Fernando Calamante, Søren Christensen, Patricia M. Desmond, Leif Østergaard, Stephen M. Davis and Alan Connelly

*Stroke*. 2010;41:1169-1174; originally published online April 22, 2010;  
doi: 10.1161/STROKEAHA.110.580670

*Stroke* is published by the American Heart Association, 7272 Greenville Avenue, Dallas, TX 75231  
Copyright © 2010 American Heart Association, Inc. All rights reserved.  
Print ISSN: 0039-2499. Online ISSN: 1524-4628

The online version of this article, along with updated information and services, is located on the  
World Wide Web at:

<http://stroke.ahajournals.org/content/41/6/1169>

**Permissions:** Requests for permissions to reproduce figures, tables, or portions of articles originally published in *Stroke* can be obtained via RightsLink, a service of the Copyright Clearance Center, not the Editorial Office. Once the online version of the published article for which permission is being requested is located, click Request Permissions in the middle column of the Web page under Services. Further information about this process is available in the [Permissions and Rights Question and Answer](#) document.

**Reprints:** Information about reprints can be found online at:  
<http://www.lww.com/reprints>

**Subscriptions:** Information about subscribing to *Stroke* is online at:  
<http://stroke.ahajournals.org/subscriptions/>